

# Theoretical basis for the measurement of local transverse dispersion in isotropic porous media

O. A. Cirpka<sup>1</sup> and P. K. Kitanidis

Department of Civil and Environmental Engineering, Stanford University, Stanford, California

**Abstract.** Spreading of a conservative solute in potential flow in a helical porous medium is dominated by the radial velocity distribution within the domain. Higher velocities at the inside of the helix compared to the outside leads to spreading that is balanced by transverse pore-scale dispersion. The angular moments of the concentration distribution exhibit the typical behavior of Taylor-Aris dispersion in which the rate of change of the second central moment is inversely proportional to pore-scale transverse dispersion. We present numerical results for the angular moments over the entire time range and derive analytical expressions for the angular macrodispersion coefficient at the large time limit. We propose a method in which macrodispersion is measured in a helix filled with the porous material of interest in order to infer pore-scale transverse dispersivity values that are difficult to determine with existing methods.

## 1. Introduction

Consider a helical domain, depicted in Figure 1, that idealizes a laboratory device that is filled with a saturated porous medium. Apply a head difference between the inlet and outlet. The resulting flow field has, owing to the geometry, higher angular velocities at the inside of the spiral than at the outside. When a conservative solute is introduced, the velocity differences lead to angular spreading of the solute. The resulting angular macrodispersion is similar to the dispersion in a capillary tube analyzed by Taylor [1953] and Aris [1956].

The motivation for this study is to develop a novel procedure for the measurement of pore-scale transverse dispersion parameters which are difficult to obtain with current methods. Pore-scale transverse dispersion has been identified as a key factor in the dilution of solutes and the mixing of reactants in porous media [Kitanidis, 1994; Kapoor and Kitanidis, 1996, 1998; Cirpka and Kitanidis, 2000; Oya and Valocchi, 1998; Kapoor and Gelhar, 1994; Fiori and Dagan, 2000; Attinger et al., 1999]. In steady-state potential flow fields, local transverse dispersion is the only process exchanging solute mass between fast and slow stream tubes. Whereas the spatial variability of advective velocities leads to highly irregular concentration fronts, transverse dispersion smooths the concentration distribution. At the large time limit, transverse dispersion eliminates the concentration variance, and the description of solute transport by macroscopic uniform parameters becomes accurate, even for initially small plumes in heterogeneous fields [Kapoor and Gelhar, 1994; Oya and Valocchi, 1998; Attinger et al., 1999; Fiori and Dagan, 2000]. According to Kapoor and Kitanidis [1998], the time that needs to elapse before the concentration variance vanishes is inversely proportional to the pore-scale transverse dispersion coefficient.

Experimental studies in the early sixties indicated local

transverse dispersivity values,  $\alpha_t$ , in the range of a few percent of the average grain size [Blackwell, 1962; Perkins and Johnston, 1963]. Bear [1972] reported the ratio between the longitudinal and the transverse local dispersivity to range between 5 and 30. For large-time macrodispersivities the ratio is much wider, since the longitudinal macrodispersivity is commonly orders of magnitudes larger than the local values whereas the transverse dispersivity hardly increases with scale [Gelhar and Axness, 1983].

### 1.1. Existing Methods for the Measurement of Transverse Dispersion

Transverse dispersion coefficients are typically evaluated by the interpretation of steady-state transverse concentration profiles of conservative solutes in parallel flow. Two miscible fluids may be introduced into parallel layers of a rectangular laboratory device [Grane and Gardner, 1961; Simpson, 1962; Perkins and Johnston, 1963; Harleman and Rumer, 1963] or into the annulus and core of a laboratory column [Blackwell, 1962; Hassinger and Rosenberg, 1968]. The transverse dispersion coefficients are then inferred from the measurements of the mixing at some distance downgradient from the entrance. As alternatives, Nishigaki et al. [1996] used line sources, and Robbins [1989] point sources of a tracer solution. Perkins et al. [1965] modified the scheme by using a point source in a sector of a radially divergent flow field. The tracer may also be injected instantaneously rather than continuously, and either the concentration distribution at a given time or the breakthrough curves at fixed locations may be used for interpretation. Transverse dispersion coefficients have been inferred from transient transport in columns [Robbins, 1989], in parallel flow [Zou and Parr, 1993, 1994; Pisani and Tosi, 1994], and in interwell tracer tests [Chen et al., 1999]. Robbins [1989] showed that the transverse dispersion coefficients evaluated from transient data are less accurate than those determined at steady state.

Most of the methods mentioned above require very accurate measurements of the concentration profile transverse to the direction of flow, and the spatial resolution should not exceed a few millimeters [Grane and Gardner, 1961; Simpson, 1962; Perkins and Johnston, 1963; Harleman and Rumer, 1963; Perkins et al., 1965; Nishigaki et al., 1996]. The concentration

<sup>1</sup>Now at Universität Stuttgart, Institut für Wasserbau, Stuttgart, Germany.

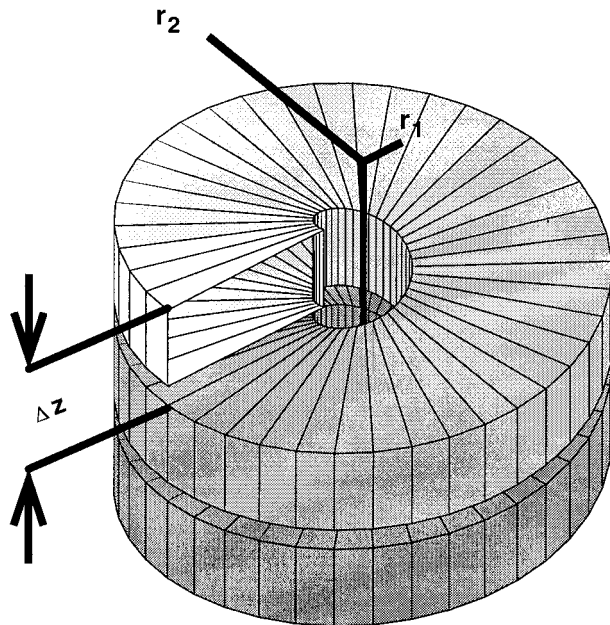


Figure 1. Visualization of the helical domain.

profiles may be distorted owing to slight heterogeneity in hydraulic conductivity leading to nonrectilinear flow. The sensitivity of the evaluated transverse dispersivity with respect to small-scale heterogeneities is extremely high for methods that are based on concentration measurements at isolated points [Robbins, 1989; Zou and Parr, 1993; Pisani and Tosi, 1994]. The same holds for the interpretation of spatially integrated concentration data such as the concentrations in the annulus and core of a column outlet [Blackwell, 1962; Hassinger and Rosenberg, 1968] or in extraction wells [Chen et al., 1999]. Small-scale heterogeneities shift the center-line of the concentration profiles. The resulting differences between the concentrations observed and those of the analytical solution which are based on ideal conditions, may lead to erroneous evaluations of the transverse dispersion coefficients.

## 1.2. Taylor-Aris Dispersion

Taylor [1953] was the first to analyze the relationship between the longitudinal dispersion coefficient for transport of a solute averaged over the cross section of a capillary tube and the molecular diffusion coefficient. The approach was extended rigorously by Aris [1956] who introduced the method of moments. Taylor-Aris dispersion is caused by the radial velocity profile in a capillary tube, which is parabolic in laminar flow. Molecular diffusion leads to an exchange in the radial direction making each particle sample all velocities with the same probability in the long term. The interaction between advective spreading in the axial direction and diffusive mixing in the radial leads to a transport behavior of the cross-sectionally averaged concentration that can be described by a one-dimensional advection-dispersion equation in which the macroscopic velocity is the arithmetic mean and the axial macrodispersion coefficient is proportional to the mean velocity squared and the inverse of the molecular diffusion coefficient.

Aris [1956] analyzed the capillary dispersion problem by the evolution of axial moments of the concentration distribution, distinguishing between what Brenner [1980b] later called global and local moments. Global moments are obtained through

integration of the concentration over the entire volume of the tube, whereas local moments are obtained through integration exclusively over the axial direction. It turns out that the temporal change of the  $k$ th global moment is the integral of an algebraic expression containing the  $(k - 1)$ th local moment, which is governed by a partial differential equation (pde) depending on the  $(k - 1)$ th global moment. The macrotransport parameters are then given by

$$v_* = \frac{1}{M_0} \frac{dM_1}{dt} \quad (1)$$

$$D_* = \frac{1}{2M_0} \frac{dM_{2c}}{dt} \quad (2)$$

in which  $v_*$  and  $D_*$  are the macroscopic velocity and dispersion coefficient,  $M_k$  is the  $k$ th global moment and  $M_{2c}$  is the second central moment. By solving the moment generating equations analytically, Aris [1956] found for transport in Poiseuille flow:

$$v_* = \frac{Q}{\pi R^2} \quad (3)$$

$$D_* = D + \frac{R^2 v_*^2}{48D} \quad (4)$$

in which  $Q$  and  $R$  are the discharge and radius of the tube, respectively, and  $D$  is the molecular diffusion coefficient. Equation (4) can be used to infer the molecular diffusion coefficient from the breakthrough curve of the cross-sectionally averaged concentration at the end of a capillary tube [Bello et al., 1994; Belongia and Baygents, 1997]. The inverse relationship between the macrodispersion coefficient  $D_*$  and  $D$  makes the approach attractive, since the molecular diffusion coefficient is very small, so that  $D_*$  is rather high and accurately detectable.

Taylor-Aris dispersion has been described for a variety of macrotransport problems, some of which are recapitulated by Brenner and Edwards [1993]. Brenner [1980a] analyzed transport of solutes in porous media represented by a spatially periodic pore network. Brenner [1980b] extended the concept of Taylor-Aris dispersion to a general macrotransport theory for systems in which global and local coordinates can be identified. For example, Brenner's theory was applied by Nadim [1988] to particle dispersion in a rotational flow field. Kitanidis [1992] and Wang and Kitanidis [1999] applied the method of moments to solute transport in groundwater with a spatially periodic or stationary field of Darcy-scale velocities.

In the present study we evaluate the spreading of solutes in helical flow in homogeneous isotropic porous media. We analyze the dependency of the angular macrodispersion coefficient on pore-scale transverse dispersion parameters. We suggest that dispersion experiments in a helical device may be used to identify the transverse dispersion parameters of the porous medium.

## 2. Flow and Transport in a Helical Porous Medium

Consider a helical domain as shown in Figure 1. The domain is characterized by the inner and outer radius  $r_1$  and  $r_2$ , the pitch  $\Delta z$ , and the number of convolutions  $n$ . If we apply a head difference between the inlet and outlet cross sections, the re-

sulting flow will be in the tangential direction, winding from the inlet to the outlet. We consider quantities that are averaged over the thickness of one whorl. For further simplification, we assume that  $\Delta z$  is negligible in comparison to the radii so that the path length of one rotation is approximated by  $2\pi r$  rather than  $\sqrt{4\pi^2 r^2 + \Delta z^2}$ . Thus the flow is viewed as two-dimensional.

Consider an extensive quantity  $P$  with density  $\rho$ . The flux-density vector of  $P$  is  $\dot{\mathbf{P}}$ . Then, the conservation of  $P$  in a two-dimensional domain described in polar coordinates is

$$\frac{\partial \rho}{\partial t} + \frac{1}{r} \frac{\partial \dot{P}_\varphi}{\partial \varphi} + \frac{\partial \dot{P}_r}{\partial r} + \frac{\dot{P}_r}{r} = 0 \quad (5)$$

in which  $r$  and  $\varphi$  are the radial and angular coordinates. It is noteworthy that the helix would simplify to a ring if the pitch  $\Delta z$  were exactly zero. In a ring,  $\varphi$  could range only from 0 to  $2\pi$ . For a small pitch  $\Delta z > 0$ , however, many rotations are possible without revisiting the same location. In our theoretical analysis, the helix is infinite and  $\varphi$  ranges from  $-\infty$  to  $+\infty$ .

In single-phase flow in porous media, the extensive quantity to be conserved is the volume of water, and the flux-density is the specific discharge  $\mathbf{q}$ , which is determined by Darcy's law:

$$q_r = -K \frac{\partial h}{\partial r} \quad (6)$$

$$q_\varphi = -\frac{K}{r} \frac{\partial h}{\partial \varphi} \quad (7)$$

in which  $h$  is the hydraulic head and  $K$  is the hydraulic conductivity. Substituting (6) and (7) into (5) and neglecting the temporal derivative yields the single-phase flow equation in porous media in polar coordinates at steady state:

$$\frac{K}{r^2} \frac{\partial^2 h}{\partial \varphi^2} + K \frac{\partial^2 h}{\partial r^2} + \frac{K}{r} \frac{\partial h}{\partial r} = 0. \quad (8)$$

For flow in a helix with constant head along the inflow and outflow radii, we get a head distribution that is constant with  $r$  and changes linearly with  $\varphi$ :

$$h(\varphi) = h_i + \frac{h_o - h_i}{\varphi_o - \varphi_i} (\varphi - \varphi_i) = h_i - J(\varphi - \varphi_i) \quad (9)$$

in which the subscripts  $i$  and  $o$  denote inflow and outflow values, respectively, and  $J$  is the negative angular head gradient. Then, the specific discharge components are

$$q_r = 0 \quad (10)$$

$$q_\varphi = \frac{KJ}{r}. \quad (11)$$

Since we consider creeping flow in porous media at the Darcy scale, inertia effects are neglected, secondary flow phenomena do not occur, and boundary effects are not observed provided that the cross section of the helix is larger than the scale of the representative elementary volume (REV) [Bear, 1972]. The total discharge  $Q_{\text{tot}}$ , the mean specific discharge  $\bar{q}$ , and the are mean rotational specific discharge  $\Omega$  are given by

$$Q_{\text{tot}} = \int_{r_1}^{r_2} q_\varphi(r) dr = KJ \ln \left( \frac{r_2}{r_1} \right) \quad (12)$$

$$\bar{q} = \frac{Q_{\text{tot}}}{r_2 - r_1} = \frac{KJ \ln \left( \frac{r_2}{r_1} \right)}{r_2 - r_1} \quad (13)$$

$$\Omega = \frac{\bar{q}}{\bar{r}} = \frac{2KJ \ln \left( \frac{r_2}{r_1} \right)}{r_2^2 - r_1^2} \quad (14)$$

in which  $\bar{r} = (r_2 + r_1)/2$  is the arithmetic average of the radius. In the corresponding transport problem, the extensive quantity  $P$  to be conserved is the mass of solute  $m$ , the volumetric density  $\rho$  is the mass over the bulk volume,  $\theta c$ , where  $c$  is the concentration in the aqueous phase, and the flux density  $\dot{\mathbf{P}}$  is the mass flux density  $\dot{\mathbf{m}}$ :

$$\theta \frac{\partial c}{\partial t} + \frac{1}{r} \frac{\partial \dot{m}_\varphi}{\partial \varphi} + \frac{\partial \dot{m}_r}{\partial r} + \frac{\dot{m}_r}{r} = 0 \quad (15)$$

in which  $\dot{m}_\varphi$  and  $\dot{m}_r$  consist of an advective and a dispersive component:

$$\dot{m}_\varphi = cq_\varphi - \theta \frac{D_\varphi}{r} \frac{\partial c}{\partial \varphi} = c \frac{KJ}{r} - \theta \frac{D_\ell}{r} \frac{\partial c}{\partial \varphi} \quad (16)$$

$$\dot{m}_r = cq_r - \theta D_r \frac{\partial c}{\partial r} = -\theta D_t \frac{\partial c}{\partial r}, \quad (17)$$

where  $D_\varphi = D_\ell$  is the tangential or longitudinal dispersion coefficient and  $D_r = D_t$  the radial or transverse one. The second equations in (16) and (17) are based on the flow field in the helix (10) and (11). Substitution of (16) and (17) into (15) yields

$$\frac{\partial c}{\partial t} + \frac{KJ}{r^2 \theta} \frac{\partial c}{\partial \varphi} - \frac{D_\ell}{r^2} \frac{\partial^2 c}{\partial \varphi^2} - \frac{\partial}{\partial r} \left( D_t \frac{\partial c}{\partial r} \right) - \frac{D_t}{r} \frac{\partial c}{\partial r} = 0. \quad (18)$$

The pore-scale dispersion coefficients for isotropic media are defined by the classical parameterization of Scheidegger [1961]:

$$D_\ell = \alpha_\ell \frac{\|\mathbf{q}\|}{\theta} + D = \alpha_\ell \frac{KJ}{r\theta} + D \quad (19)$$

$$D_t = \alpha_t \frac{\|\mathbf{q}\|}{\theta} + D = \alpha_t \frac{KJ}{r\theta} + D \quad (20)$$

in which  $\alpha_\ell$  and  $\alpha_t$  are the longitudinal and transverse dispersivities which are assumed properties of the porous medium. Note that in (19) and (20),  $D$  is the effective diffusion coefficient which may differ from the molecular by a constant factor, referred to as tortuosity. The molecular diffusion coefficients of common tracers are known; typical values are of the order of  $10^{-9}$  m<sup>2</sup>/s. The tortuosity, by contrast, is a property of the porous medium that is not known a priori. A procedure for the determination of the effective diffusion coefficient  $D$  aims therefore mainly on evaluating the tortuosity. The Scheidegger parameterization is valid at the Darcy or representative elementary volume (REV) scale [Bear, 1972]. The relaxation time associated with particles to sample the entire cross section of a pore is of the order of  $L_p^2/D \approx 10$  s, where  $L_p$  is the pore diameter that is smaller than  $10^{-4}$  m for sands. We therefore neglect single-pore effects and treat the Darcy scale, which is much larger than the scale of single pores, as the local scale.

Substitution of (19) and (20) into (18) gives

$$\frac{\partial c}{\partial t} + \frac{A}{r^2} \frac{\partial c}{\partial \varphi} - \left( \alpha_\ell \frac{A}{r^3} + \frac{D}{r^2} \right) \frac{\partial^2 c}{\partial \varphi^2} - \left( \alpha_\ell \frac{A}{r} + D \right) \frac{\partial^2 c}{\partial r^2} - \frac{D}{r} \frac{\partial c}{\partial r} = 0 \quad (21)$$

with

$$A = \frac{KJ}{\theta} \quad (22)$$

subject to the radial boundary conditions:

$$\left. \frac{\partial c}{\partial r} \right|_{r=r_1} = 0 \quad (23)$$

$$\left. \frac{\partial c}{\partial r} \right|_{r=r_2} = 0. \quad (24)$$

Additional auxiliary conditions for the angular directions and initial conditions are required to define the problem. In the following analysis, we assume an infinite helix. At the large-distance limits we require

$$\lim_{\varphi \rightarrow \pm\infty} \frac{\partial^n c(\varphi, r, t)}{\partial \varphi^n} = 0 \quad n = 0, 1, 2 \dots \quad (25)$$

We will consider two initial conditions: For the case of a Dirac-like line, we will analyze the full time range of solute transport, whereas we will restrict our analysis to the large-time behavior for arbitrary initial conditions.

### 3. Definition of Moments

We consider the behavior of the radius-weighted, cross-sectional average of the concentration  $\bar{c}$ :

$$\bar{c}(\varphi, t) = \frac{2}{r_2^2 - r_1^2} \int_{r_1}^{r_2} rc(\varphi, r, t) dr. \quad (26)$$

In analogy to transport in parallel flow, we expect that  $\bar{c}$  satisfies, after a relaxation time, a macroscopic advection-dispersion equation:

$$\frac{\partial \bar{c}}{\partial t} + \omega_{\text{mac}} \frac{\partial \bar{c}}{\partial \varphi} - D_{\text{mac}}^\varphi \frac{\partial^2 \bar{c}}{\partial \varphi^2} = 0 \quad (27)$$

in which  $\omega_{\text{mac}}$  and  $D_{\text{mac}}^\varphi$  are the macroscopic rotational seepage velocity and dispersion coefficient, respectively, both of dimension  $1/T$ . The objective of the present study is to express these macroscopic parameters in terms of the dimensions  $r_1$  and  $r_2$  of the helix, the mean rotational specific discharge  $\Omega$ , the porosity  $\theta$ , and the parameters determining pore-scale dispersion  $\alpha_\ell$ ,  $\alpha_r$ , and  $D$ . We infer the macrotransport parameters from the rate of change of the global angular moments  $M_k$  of the concentration distribution defined by

$$M_k(t) = \int_{-\infty}^{+\infty} \int_{r_1}^{r_2} \varphi^k rc(\varphi, r, t) dr d\varphi. \quad (28)$$

The zeroth global moment  $M_0$  is the total mass in the domain. In the following, we normalize the concentration  $c$  with the total mass  $M_0$ . Then the zeroth global moment  $M_0$  of the normalized concentration is unity and the first global moment  $M_1$  is the mean angular coordinate of the concentration dis-

tribution. For the second and higher moments, we also define central moments  $M_{kc}(t)$ :

$$M_{kc}(t) = \int_{-\infty}^{+\infty} \int_{r_1}^{r_2} \left( \varphi - \frac{M_1^\varphi}{M_0^\varphi} \right)^k rc(\varphi, r, t) dr d\varphi. \quad (29)$$

The second central moment describes the spread of the concentration distribution with respect to the angular coordinate. The following identity of the second central moment is useful:

$$M_{2c} = M_2 - M_1^2. \quad (30)$$

If (27) is valid, we can relate the temporal derivatives of the global moments to the macroscopic parameters  $\omega_{\text{mac}}$  and  $D_{\text{mac}}^\varphi$  by

$$\frac{dM_0}{dt} = 0 \quad (31)$$

$$\frac{dM_1}{dt} = \omega_{\text{mac}} \quad (32)$$

$$\frac{dM_{2c}}{dt} = 2D_{\text{mac}}^\varphi. \quad (33)$$

Following the approach of *Aris* [1956], we additionally define local angular moments that depend only on the radial (local) but not on the angular (global) coordinate:

$$m_k(r, t) = \int_{-\infty}^{+\infty} \varphi^k c(\varphi, r, t) d\varphi. \quad (34)$$

Obviously, the global moments  $M_k$  can be calculated from the corresponding local moments  $m_k$  by radius-weighted integration:

$$M_k(t) = \int_{r_1}^{r_2} rm_k(r, t) dr. \quad (35)$$

### 4. Moment-Generating Equations for a Line Source as Initial Distribution

Consider the initial condition

$$c(\varphi, r, t_0) = c_0 \delta(\varphi - \varphi_0) \quad (36)$$

in which  $\varphi_0$  is the angular position of the line source. Without loss of generality, we chose our system of coordinates such that  $\varphi_0 = 0$ . Then the local moments at the initial state are

$$m_0(r, t_0) = \frac{2}{r_2^2 - r_1^2} \quad (37)$$

$$m_1(r, t_0) = 0 \quad (38)$$

$$m_{2c}(r, t_0) = 0. \quad (39)$$

#### 4.1. Zeroth Moment

Integrating (21) over  $\varphi$  and applying the divergence theorem, gives the governing pde for the local zeroth moment  $m_0$ :

$$\frac{\partial m_0}{\partial t} - \left( \alpha_\ell \frac{A}{r} + D \right) \frac{\partial^2 m_0}{\partial r^2} - \frac{D}{r} \frac{\partial m_0}{\partial r} = 0 \quad (40)$$

$$\left. \frac{\partial m_0}{\partial r} \right|_{r=r_1} = 0 \quad (41)$$

$$\left. \frac{\partial m_0}{\partial r} \right|_{r=r_2} = 0. \quad (42)$$

Since  $m_0$  is uniformly distributed at the initial state, all radial derivatives are zero, and  $m_0$  does not change with time.

#### 4.2. First Moment

Multiplying (21) with  $\varphi$ , integrating over  $\varphi$  and applying the divergence theorem and Green's theorem, gives the governing pde for the local first moment  $m_1$ :

$$\frac{\partial m_1}{\partial t} - \left( \alpha_t \frac{A}{r} + D \right) \frac{\partial^2 m_1}{\partial r^2} - \frac{D}{r} \frac{\partial m_1}{\partial r} = \frac{A}{r^2} m_0 \quad (43)$$

$$\left. \frac{\partial m_1}{\partial r} \right|_{r=r_1} = 0 \quad (44)$$

$$\left. \frac{\partial m_1}{\partial r} \right|_{r=r_2} = 0. \quad (45)$$

Substituting the uniform value of  $m_0$  regarding to (37) into (43) yields

$$\frac{\partial m_1}{\partial t} - \left( \alpha_t \frac{A}{r} + D \right) \frac{\partial^2 m_1}{\partial r^2} - \frac{D}{r} \frac{\partial m_1}{\partial r} = \frac{A}{r^2} \frac{2}{r_2^2 - r_1^2}. \quad (46)$$

Multiplying (46) by  $r$  and integrating the resulting expression over  $r$ , we retrieve the governing equation for the global first moment  $M_1$ :

$$\begin{aligned} \frac{dM_1}{dt} - \int_{r_1}^{r_2} (\alpha_t A + rD) \frac{\partial^2 m_1}{\partial r^2} dr - \int_{r_1}^{r_2} D \frac{\partial m_1}{\partial r} dr \\ = \frac{2A \ln \left( \frac{r_2}{r_1} \right)}{(r_2^2 - r_1^2)}. \end{aligned} \quad (47)$$

Applying Green's theorem to the first integral, we arrive at

$$\begin{aligned} \frac{dM_1}{dt} + \int_{r_1}^{r_2} D \frac{\partial m_1}{\partial r} dr \\ - \underbrace{\left[ (\alpha_t A + Dr) \frac{\partial m_1}{\partial r} \right]_{r_1}^{r_2}}_{=0} - \int_{r_1}^{r_2} D \frac{\partial m_1}{\partial r} dr \\ = \frac{2A \ln \left( \frac{r_2}{r_1} \right)}{(r_2^2 - r_1^2)} \end{aligned} \quad (48)$$

in which the radial boundary conditions (44) and (45) have been considered. Obviously, the two integrals in (48) cancel each other:

$$\frac{dM_1}{dt} = \frac{2A \ln \left( \frac{r_2}{r_1} \right)}{r_2^2 - r_1^2} = \frac{2A \ln \left( \frac{r_2}{r_1} \right)}{(r_2 - r_1)(r_2 + r_1)} = \frac{\bar{q}}{\theta \bar{r}} = \frac{\Omega}{\theta} = \omega \quad (49)$$

in which  $\omega = \bar{q}/(\theta \bar{r})$  is the mean rotational seepage velocity which is, obviously, identical to the macroscopic rotational seepage velocity  $\omega_{\text{mac}}$ . Since the first global moment is zero at the initial state,  $M_1(t)$  is given by

$$M_1(t) = \omega t. \quad (50)$$

On the basis of (50), we can express the local first moment  $m_1$  as the sum of a trend that depends linearly on time and is uniform in the radial coordinate, and a deviation  $m_0 b(r, t)$  that approaches a time-invariant profile at the large-time limit:

$$m_1(r, t) = m_0[\omega t + b(r, t)]. \quad (51)$$

Substitution into the definition of the first global moment  $M_1(t)$  yields

$$M_1(t) = m_0 \omega t \int_{r_1}^{r_2} r dr + m_0 \int_{r_1}^{r_2} r b(r, t) dr. \quad (52)$$

Considering (50), the second integral equals zero:

$$\int_{r_1}^{r_2} r b(r, t) dr = 0. \quad (53)$$

Substituting (51) into (46) yields the governing pde for the normalized deviation  $b$ :

$$\frac{\partial b}{\partial t} - \left( \alpha_t \frac{A}{r} + D \right) \frac{\partial^2 b}{\partial r^2} - \frac{D}{r} \frac{\partial b}{\partial r} = \frac{A}{r^2} - \omega \quad (54)$$

$$\left. \frac{\partial b}{\partial r} \right|_{r=r_1} = 0 \quad (55)$$

$$\left. \frac{\partial b}{\partial r} \right|_{r=r_2} = 0 \quad (56)$$

$$b(r, t_0) = 0. \quad (57)$$

It may be noted that the analytical solution of (54) by solving the related eigenvalue-eigenfunction problem requires that a solvability condition is met [Barton, 1983] [see also Aris, 1999, pp. 67–68]. In section 6, we will consider only the large-time behavior of  $b$  so that (54) simplifies to an ordinary differential equation that can be solved without the condition of Barton [1983].

#### 4.3. Second Noncentral and Central Moment

Multiplying (21) with  $\varphi^2$ , integrating over  $\varphi$ , and applying the divergence theorem and Green's theorem, gives the governing pde for the local second moment  $m_2$ :

$$\begin{aligned} \frac{\partial m_2}{\partial t} - \left( \alpha_t \frac{A}{r} + D \right) \frac{\partial^2 m_2}{\partial r^2} - \frac{D}{r} \frac{\partial m_2}{\partial r} \\ = 2 \frac{A}{r^2} m_1 + 2 \left( \alpha_t \frac{A}{r^3} + \frac{D}{r^2} \right) m_0 \end{aligned} \quad (58)$$

$$\left. \frac{\partial m_2}{\partial r} \right|_{r=r_1} = 0 \quad (59)$$

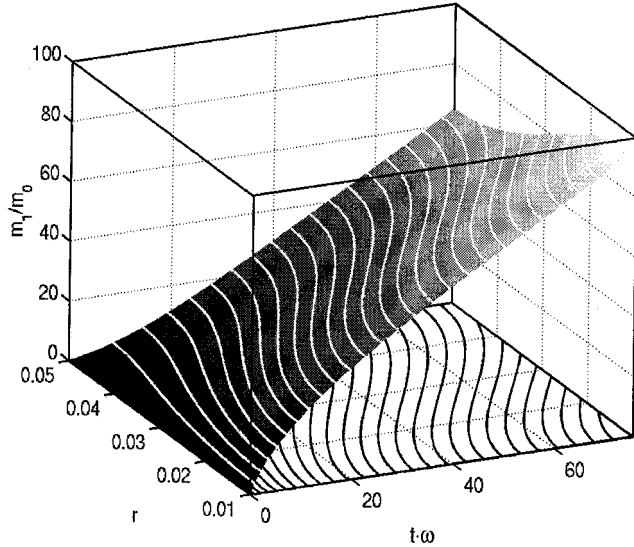


**Figure 2.** First local moment as function of time and radial coordinate:  $r_1 = 0.01$  m,  $r_2 = 0.05$  m,  $\alpha_r = 5 \times 10^{-4}$  m,  $\alpha_e = 1 \times 10^{-3}$  m,  $\theta = 0.33$ ,  $J = 1 \times 10^{-3}/(2\pi)$  m,  $D = 0$  m<sup>2</sup>/s.

$$\left. \frac{\partial m_2}{\partial r} \right|_{r=r_2} = 0. \quad (60)$$

Multiplication with and integration over  $r$  yields the governing equation for the second global moment. After applying the same transformation rules as for the first moment, we get

$$\begin{aligned} \frac{dM_2}{dt} &= 2 \int_{r_1}^{r_2} \frac{A}{r} m_1 dr + \left[ \alpha_e A \left( \frac{1}{r_1} - \frac{1}{r_2} \right) \right. \\ &\quad \left. + D \ln \left( \frac{r_2}{r_1} \right) \right] \frac{4}{r_2^2 - r_1^2}. \end{aligned} \quad (61)$$

Evaluation of the second global moment requires the calculation of only the first local moment. This follows from the approach of *Aris* [1956] and its generalization into the macro-transport paradigm by *Brenner and Edwards* [1993] stating for any type of Taylor-Aris dispersion that the evaluation of the  $k$ th global moment requires the knowledge of the  $(k - 1)$ th local moment, whereas the  $k$ th local moment requires the knowledge of the  $k$ th global moment.

Differentiating (30) with respect to time:

$$\frac{dM_{2c}}{dt} = \frac{dM_2}{dt} - 2M_1(t) \frac{dM_1}{dt} \quad (62)$$

and substituting (61) and (50) into (62) yields:

$$\begin{aligned} \frac{dM_{2c}}{dt} &= 2 \int_{r_1}^{r_2} \frac{A}{r} m_1 dr - 2\omega^2 t \\ &\quad + \left[ \alpha_e A \left( \frac{1}{r_1} - \frac{1}{r_2} \right) + D \ln \left( \frac{r_2}{r_1} \right) \right] \frac{4}{r_2^2 - r_1^2}. \end{aligned} \quad (63)$$

From this we derive the macroscopic angular dispersion coefficient  $D_{\text{mac}}^\varphi$ :

$$\begin{aligned} D_{\text{mac}}^\varphi &= \frac{1}{2} \frac{dM_{2c}}{dt} \\ &= \underbrace{\int_{r_1}^{r_2} \frac{A}{r} m_1 dr - \omega^2 t}_{D_*^\varphi} \\ &\quad + \underbrace{\frac{2}{r_2^2 - r_1^2} \left[ \alpha_e A \left( \frac{1}{r_1} - \frac{1}{r_2} \right) + D \ln \left( \frac{r_2}{r_1} \right) \right]}_{D_\ell^\varphi} \end{aligned} \quad (64)$$

which contains the hydrodynamic macrodispersion coefficient  $D_*^\varphi$  and the specially averaged local dispersion coefficient  $D_\ell^\varphi$ . In most practical applications the former significantly exceeds the latter. After some rearrangements, we can simplify the hydrodynamic term  $D_*^\varphi$  by

$$D_*^\varphi = \frac{\omega}{\ln \left( \frac{r_2}{r_1} \right)} \int_{r_1}^{r_2} \frac{b(r)}{r} dr. \quad (65)$$

That is,  $D_*^\varphi$  can be evaluated from the normalized deviation  $b$  of the first moment  $m_1$ . At early times,  $D_*^\varphi$  is time dependent, and  $\bar{c}$  does not satisfy (27). Nevertheless,  $D_*^\varphi$ , i.e., half the rate of change of the second central moment, is known as time-dependent macrodispersion [*Dagan*, 1988; *Gelhar et al.*, 1992]. Note that (65) depends directly on  $b(r)$ . It is equivalent to (4.25) in the general approach of *Brenner* [1980b] for the large-time behavior. Owing to the initial condition (36),  $m_0$  is uniformly distributed at all times, and (65) holds also at early times. Multiplying (54) with  $rb$ , applying identities of differentiation, integrating over  $r$ , considering the boundary conditions (55) and (56), identity (53) and the definition of  $\omega$  (49) yields after comparison with (65):

$$D_*^\varphi = m_0 \int_{r_1}^{r_2} rb \frac{\partial b}{\partial t} dr + m_0 \int_{r_1}^{r_2} r \left( \frac{\partial b}{\partial r} \right)^2 \left( \alpha_e \frac{A}{r} + D \right) dr. \quad (66)$$

At the large-time limit,  $b$  approaches steady state and the first integral of (66) vanishes. Canceling the first integral, (66) is identical to (4.29) in the general approach of *Brenner* [1980b], applied to our specific system. *Nadim* [1988] adopted Brenner's method for the determination of isotropic particle diffusion by angular dispersion experiments in a Couette device; *Nadim* derived (66) without the first integral and without the local dispersion contribution  $\alpha_e A/r$  by applying Brenner's general approach. At the large-time limit, (66) requires only the derivative of  $b$  with respect to  $r$ , whereas (65) depends directly on  $b$ . At early times, both expressions are exact for the given initial condition (36). By contrast, *Brenner* [1980b] represented the early-time behavior by an exponentially decaying term that depends on the exact initial condition.

Equations (65) and (66) are identical expressions, and preferring one over the other depends on the way how  $b(r)$  and  $D_*^\varphi$  are evaluated. If the governing pde (54) is solved analytically, expression (66) is advantageous because  $b(r)$  may be determined to an unknown constant. This constant, however, is given by constraint (53). If (54) is solved by a numerical approach, (65) is advantageous because the derivative  $\partial b/\partial r$ ,

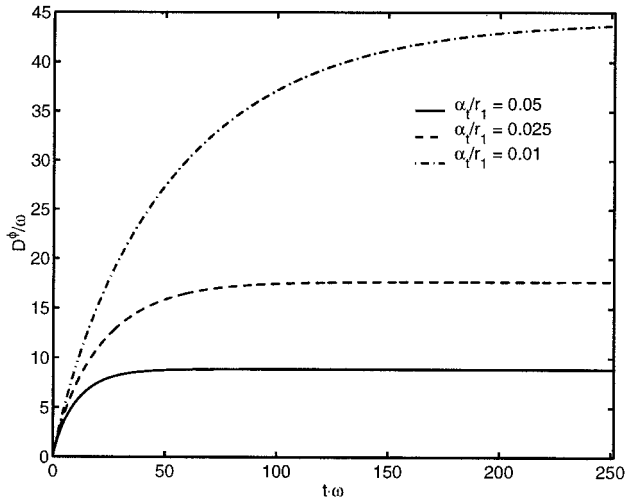


**Figure 3.** Angular hydrodynamic dispersion coefficient as function of time and different dimensionless local-scale transverse dispersivities  $\bar{\alpha}_t = \alpha_t/r_1$ .  $\bar{R} = r_2/r_1 = 5$ . Molecular diffusion is neglected.

required for (66), will be approximated less accurately than  $b(r)$ , required by (65).

## 5. Numerical Results

Equation (43) was solved numerically using a standard Finite Element Method applying a wide range of parameters. All simulations showed identical qualitative behavior. At early times, the first local moment increases much faster at the inside of the helix than at the outside since the velocity is higher. This leads to an increasing radial gradient inducing a first-moment flux from the inside to the outside. At large times, the radially varying source and the flux due to transverse dispersion are balanced, and the temporal increase of the first moment becomes identical for all radial coordinates. The temporal development of the first local moment distribution for one set of parameters is shown in Figure 2. Equation (36) was

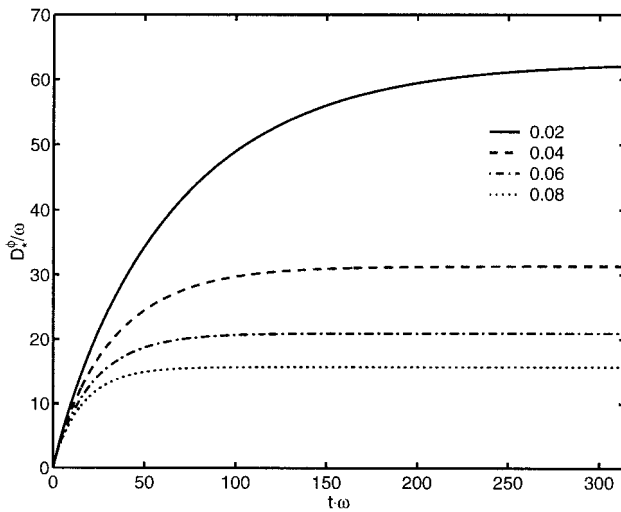


**Figure 4.** Angular hydrodynamic dispersion coefficient as function of time and different dimensionless molecular diffusion coefficients  $\bar{D}_m = D/(r_1^2\omega)$ .  $\bar{R} = r_2/r_1 = 5$ . Velocity-proportional, pore-scale dispersion is neglected.

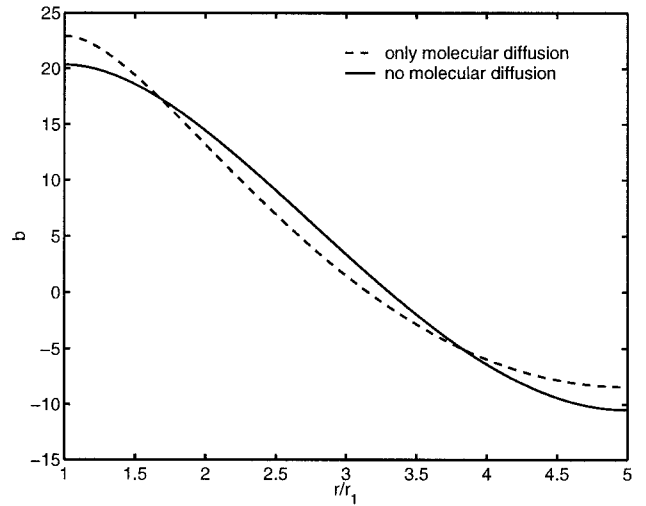


**Figure 5.** Large-time profile of the deviation  $b$  from the local first moment  $m_1$ . Comparison between the case neglecting velocity-proportional, pore-scale dispersion ( $\bar{D}_m = 0.1422$ ) and that neglecting molecular diffusion ( $\bar{\alpha}_t = 0.05$ ) leading to identical angular macrodispersion. Radius ratio  $\bar{R} = 5$ .

chosen as initial condition. Molecular diffusion was neglected in this particular simulation.

Equation (64) was used to calculate the time-dependent angular macrodispersion coefficient  $D_{\text{mac}}^\varphi$ . Figure 3 shows model results of  $D_{\text{mac}}^\varphi/\omega$  for various transverse dispersivity values neglecting molecular diffusion. At the large-time limit the angular macrodispersion coefficients are approximately inverse proportional to the pore-scale transverse dispersivity values. For  $\alpha_t/r_1 = 0.05$ , a dimensionless time of  $t\omega \approx 8 \times 2\pi$  is needed to approach the large-time limit. The dimensionless characteristic time for approaching steady state appears to be proportional to the value of  $D_{\text{mac}}^\varphi/\omega$  at the large-time limit. Note that for the parameters chosen, the normalized local contribution to macrodispersion  $D_\ell^\varphi/\omega$  is 0.05 and therefore negligible compared to the hydrodynamic contribution  $D_\#^\varphi/\omega$ .

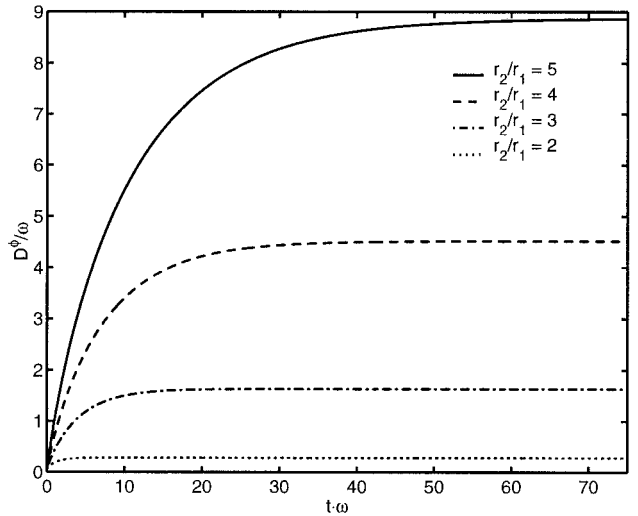


**Figure 6.** Angular hydrodynamic dispersion coefficient as function of time and different ratios of radii:  $r_1 = 0.01$  m,  $r_2$  variable,  $\alpha_t = 5 \times 10^{-4}$  m,  $\alpha_\ell = 1 \times 10^{-3}$  m,  $\theta = 0.33$ ,  $J = 1 \times 10^{-3}/(2\pi)$  m,  $D = 0$  m<sup>2</sup>/s.

Figure 4 shows model results of  $D_{\text{mac}}^\varphi/\omega$  for various dimensionless molecular diffusion coefficient neglecting velocity-proportional, pore-scale dispersion. The qualitative behavior is identical to that shown in Figure 3;  $D_{\text{mac}}^\varphi$  increases with time and approaches a constant large-time value that is inversely proportional to the pore-scale diffusion. Figure 5 shows a comparison of the large-time, first-moment profiles for the two cases considered. The parameters were chosen such that the resulting angular macrodispersion coefficients are identical. In the case considering velocity-proportional dispersion, the pore-scale transverse dispersion coefficient is higher at the inside of the helix than at the outside. Therefore the  $b$  profile shows, compared to the case in which only molecular diffusion is considered, lower values at the inside. However, the differences are not pronounced.

Figure 6 shows  $D_{\text{mac}}^\varphi/\omega$  for various ratios of the radii neglecting molecular diffusion. The larger the ratio  $\bar{R} = r_2/r_1$ , the higher the large-time angular macrodispersion coefficient  $D_{\text{mac}}^\varphi$ . This behavior is anticipated since the ratio of the fastest to the slowest velocity is that of the radii squared. The dependency of  $D_{\text{mac}}^\varphi/\omega$  on  $\bar{R}$  is not linear.

## 6. Large-Time Behavior for Arbitrary Initial Conditions

The governing equations for the zeroth local moment  $m_0$  (40)–(42), the first local moment  $m_1$  (43)–(45), and the second local moment  $m_2$  (58)–(60) are also valid for an initial distribution of  $c$  other than the line-source (36). If the solute mass is initially concentrated at a certain axial position  $r$  or spread over an angular range  $\varphi$ , the absolute values of the moments will differ at all times from the line-source solution, whereas the rate of change will differ only at early times. As time increases,  $m_0$  approaches, owing to transverse dispersion, a uniform distribution with respect to  $r$ . Then the source-term in the governing pde for the first moment  $m_1$  in (43) becomes uniform, and  $b$  approaches a steady state.

Excluding cases with infinite solute mass such as a Heaviside initial distribution,  $M_0$  is constant for the entire time range. The linear increase of the first global moment  $M_1$  (47) can be observed only at the large-time limit. The large-time absolute value of  $M_1$ , however, differs from (50) by a constant representing early-time effects. At the large-time limit, the expressions for the rate of change of the second central global moment  $M_{2c}$  and the angular macrodispersion coefficient  $D_{\text{mac}}^\varphi$  for arbitrary initial conditions are identical to those for the line-source problem (61) and (64).

The governing equation for the first-moment deviation  $b$  (54) remains unchanged for arbitrary initial conditions, if we normalize the deviation of  $m_1$  with the large-time value  $m_0^\infty$  rather than the actual value of the zeroth moment  $m_0$ . We introduce the following dimensionless quantities:

$$\bar{t} = t\omega \quad (67)$$

$$\bar{r} = \frac{r}{r_1} \quad (68)$$

$$\bar{\alpha}_t = \frac{\alpha_t}{r_1} \quad (69)$$

$$\bar{R} = \frac{r_2}{r_1} \quad (70)$$

$$\bar{v} = \frac{KJ}{\omega\theta r_1^2} = \frac{\bar{R}^2 - 1}{2 \ln(\bar{R})} \quad (71)$$

$$\bar{D} = \frac{D}{\omega r_1^2} \quad (72)$$

in which  $\bar{t}$  is a dimensionless time,  $\bar{r}$  and  $\bar{\alpha}_t$  are the radial coordinate and the transverse dispersivity normalized by the inner radius of the ring,  $\bar{R}$  is the ratio of the outer and inner radius,  $\bar{v}$  is a dimensionless velocity, and  $\bar{D}_m$  a dimensionless molecular diffusion coefficient. Equation (54) becomes now

$$\frac{\partial b}{\partial \bar{t}} - \left( \frac{\bar{\alpha}_t \bar{v}}{\bar{r}} + \bar{D} \right) \frac{\partial^2 b}{\partial \bar{r}^2} - \frac{\bar{D}}{\bar{r}} \frac{\partial b}{\partial \bar{r}} = \frac{\bar{v}}{\bar{r}^2} - 1 \quad (73)$$

$$\left. \frac{\partial b}{\partial r} \right|_{\bar{r}=1} = 0 \quad (74)$$

$$\left. \frac{\partial b}{\partial r} \right|_{\bar{r}=\bar{R}} = 0. \quad (75)$$

At the large-time limit,  $b$  approaches a steady state distribution  $b^\infty(\bar{r})$ :

$$-\left( \frac{\bar{\alpha}_t \bar{v}}{\bar{r}} + \bar{D} \right) \frac{\partial^2 b^\infty}{\partial \bar{r}^2} - \frac{\bar{D}}{\bar{r}} \frac{\partial b^\infty}{\partial \bar{r}} = \frac{\bar{v}}{\bar{r}^2} - 1 \quad (76)$$

subject to the boundary conditions (74) and (75). Note that (76) is an ordinary differential equation which can be solved analytically.

With the dimensionless quantities we may express the two contributions to the angular macrodispersion coefficient, defined in (64), in dimensionless form:

$$\frac{D_{\text{mac}}^\varphi}{\omega} = \frac{2}{\bar{R}^2 - 1} \int_1^{\bar{R}} \bar{r} \left( \frac{\partial b(\bar{r})}{\partial \bar{r}} \right)^2 \left( \frac{\bar{\alpha}_t \bar{v}}{\bar{r}} + \bar{D} \right) d\bar{r} \quad (77)$$

$$\omega = \frac{D_\ell^\varphi}{\bar{\alpha}_t} \frac{\bar{R} - 1}{\bar{R} \ln(\bar{R})} + \bar{D}_m \frac{2 \ln(\bar{R})}{\bar{R}^2 - 1}. \quad (78)$$

In the following, we present analytical results of the large-time angular macrodispersion coefficient in dimensionless terms for two simplifying cases: (a) “no molecular diffusion” in which transverse pore-scale dispersion is fully described by a velocity-proportional term; and (b) “only molecular diffusion” where the transverse pore-scale dispersion coefficient is constant for all velocities. A complete description of pore-scale dispersion would be given by the sum of a velocity-dependent and independent term. Since the corresponding analytical results of  $D_{\text{mac}}^\varphi$  is rather complicated, we suggest a simpler approximation.

### 6.1. No Molecular Diffusion

The analytical solution of (76) subject to the boundary conditions (74) and (75) is for  $\bar{D}_m = 0$ :

$$b^\infty(\bar{r}) =$$

$$\frac{1/3 \ln(\bar{R})\bar{r}^3 - \bar{R}^2 \bar{r} \ln(\bar{r}) + \bar{R}^2 \bar{r} + \bar{r} \ln(\bar{r}) - \bar{r} - \ln(\bar{R})\bar{r}}{\bar{\alpha}_t(\bar{R}^2 - 1)} + C \quad (79)$$

in which  $C$  is an integration constant that can be determined by the auxiliary condition (53) but is not needed. Substituting (79)

into (77) yields the analytical solution for the hydrodynamic contribution to the angular macrodispersion coefficient:

$$\begin{aligned} \frac{D_*^\varphi}{\omega} = & \frac{16}{9} \frac{(-\bar{R}^4 - \bar{R}^3 + \bar{R} + 1)}{\bar{\alpha}_t(\bar{R}^3 + \bar{R}^2 - \bar{R} - 1)} \\ & + \frac{8}{15} \frac{\ln(\bar{R})(\bar{R}^4 + \bar{R}^3 + \bar{R}^2 + \bar{R} + 1)}{\bar{\alpha}_t(\bar{R}^3 + \bar{R}^2 - \bar{R} - 1)} \\ & + \frac{2\bar{R}^4 - 4\bar{R}^2 + 2}{\bar{\alpha}_t(\bar{R}^3 + \bar{R}^2 - \bar{R} - 1)\ln(\bar{R})}. \end{aligned} \quad (80)$$

The hydrodynamic contribution to the angular macrodispersion coefficient  $D_*^\varphi$  is inversely proportional to the pore-scale dispersivity  $\alpha_t$ . As indicated earlier, typical values for  $\alpha_t$  are very small leading to large values of  $D_*^\varphi$ . Since neither the ratio of radii  $\bar{R}$  nor the dimensionless transverse dispersivity  $\bar{\alpha}_t$  depend on the velocity,  $D_*^\varphi$  is proportional to the mean rotational seepage velocity  $\omega$ . This behavior is anticipated since macrodispersion coefficients in Taylor-Aris dispersion are typically proportional to the velocity squared divided by the transverse dispersion coefficient which is in the case considered proportional to the velocity.

### 6.2. Only Molecular Diffusion

The analytical solution of (76) subject to the boundary conditions (74) and (75) is for  $\bar{\alpha}_t = 0$ :

$$b^z(\bar{r}) = \frac{[\ln(\bar{r})]^2 + \ln(\bar{R})\bar{r}^2 - \bar{R}^2[\ln(\bar{r})]^2}{4\bar{D}\ln(\bar{R})} - \frac{\ln(\bar{r})}{2\bar{D}} + C. \quad (81)$$

Substituting (81) into (77) yields the analytical solution for the hydrodynamic contribution to the angular macrodispersion coefficient:

$$\begin{aligned} \frac{D_*^\varphi}{\omega} = & \frac{\ln(\bar{R})(\bar{R}^4 + \bar{R}^2 + 1)}{6\bar{D}(\bar{R}^2 - 1)} \\ & + \frac{3\ln(\bar{R})(-\bar{R}^4 + 1) + 2\bar{R}^4 - 4\bar{R}^2 + 2}{8\bar{D}\ln(\bar{R})(\bar{R}^2 - 1)}. \end{aligned} \quad (82)$$

Similarly to (80), the analytical solution considering molecular diffusion as the only transverse mixing process (82) exhibits an inverse relationship between pore-scale transverse dispersion and macroscopic angular dispersion. However, since  $\bar{D}$  is already normalized by the mean rotational velocity  $\omega$ , the dimensional hydrodynamic contribution to the angular macrodispersion coefficient  $D_*^\varphi$  is proportional to  $\omega^2$  as expected from classical Taylor-Aris dispersion [Taylor, 1953; Aris, 1956].

### 6.3. Both Velocity-Proportional Dispersion and Molecular Diffusion

Considering both velocity-proportional dispersivity and molecular diffusion, the analytical result of  $D_*^\varphi/\omega$  becomes a rather lengthy expression containing several polylogarithmic-function terms. We use an approximation considering that the velocity-proportional dispersivity and molecular diffusion are additive at the local scale, and the macrodispersion coefficient is inversely proportional to the local-scale dispersion:

$$D_*^\varphi \propto \frac{1}{D + \bar{v}\alpha_t} \quad (83)$$

in which  $\bar{v}$  is the average seepage velocity. Therefore we may approximate the macrodispersion considering both local-scale dispersion processes by

$$\frac{D_*^\varphi}{\omega}(\bar{D}, \bar{\alpha}_t) \approx \left\{ \left[ \frac{D_*^\varphi}{\omega}(\bar{D}, 0) \right]^{-1} + \left( \frac{D_*^\varphi}{\omega}(0, \bar{\alpha}_t) \right)^{-1} \right\}^{-1} \quad (84)$$

in which  $D_*^\varphi/\omega(\bar{D}, 0)$  and  $D_*^\varphi/\omega(0, \bar{\alpha}_t)$  are the analytical expressions for the normalized angular macrodispersion coefficient neglecting velocity-proportional dispersion or molecular diffusion, respectively. We have tested the approximation (84) numerically over a wide range of parameters and found the error smaller than 1%.

## 7. Conclusions

In the present study we have analyzed Taylor-Aris dispersion in a helical porous medium. The helical geometry enforces a velocity profile that varies in a well-defined way with the radial coordinate. The spatial variability leads to advective spreading of a conservative solute. Without pore-scale transverse dispersion, the second central spatial moment would increase with time squared. The transverse exchange due to pore-scale dispersion limits the increase of the second central moment to a time-proportional process. At the large-time limit, the rate of change becomes inversely proportional to the pore-scale transverse dispersion coefficient.

We have simulated the early-time behavior of the angular second moment with a numerical model, and we have developed analytical results for the large-time limit adopting the method of moments by Aris [1956] to transport in a potential flow field in a helical geometry. It should be noted that the classical setup for macrodispersion in a straight tube as analyzed by Taylor [1953] and Aris [1956] is not applicable to porous media since the underlying parabolic velocity profile does not evolve in a packed column. In a straight tube, the Darcy-scale velocities analyzed in the present study would be uniformly distributed. Thus, for Darcy-flow, the helical geometry is instrumental in creating parallel stream tubes with a velocity-distribution increasing transverse to the direction of flow.

Traditional methods for the measurement of pore-scale transverse dispersion coefficients require extremely accurate measurements of concentration profiles transverse to the direction of flow. They are based on measuring effects that are proportional to the quantity of interest. By contrast, the angular macrodispersion coefficient in a helical porous medium is inversely proportional to the pore-scale transverse dispersion parameters. The inverse relationship is advantageous since the quantity of interest is very small. We propose therefore to measure the angular macrodispersion coefficient  $D_{\text{mac}}^\varphi$  at various mean velocities. Then the contributions of velocity-proportional and velocity-independent transverse dispersion to  $D_*^\varphi$  can be identified by inverting (84), and pore-scale transverse dispersivity  $\alpha_t$  as well as the effective molecular diffusion coefficient  $D$  can be solved by (79) and (81).

**Acknowledgments.** This study is made possible by the research scholarship "Scaling effects of in-situ mixing in heterogeneous aquifers" of the Deutsche Forschungsgemeinschaft under the grant Ci 26/3-1. Additional funding was provided by EPA through the Western Region Hazardous Substance Research Center, project SU99-9. We

want to thank Vivek Kapoor, Rutherford Aris, and Sabine Attinger for their helpful comments.

## References

- Aris, R., On the dispersion of a solute in a fluid flowing through a tube, *Proc. R. Soc. London, Ser. A*, 235, 67–77, 1956.
- Aris, R., *Mathematical Modeling: A Chemical Engineer's Perspective*, Academic, San Diego, Calif., 1999.
- Attinger, S., M. Dentz, H. Kinzelbach, and W. Kinzelbach, Temporal behaviour of a solute cloud in a chemically heterogeneous porous medium, *J. Fluid Mech.*, 386, 77–104, 1999.
- Barton, N. G., On the method of moments for solute dispersion, *J. Fluid Mech.*, 126, 205–218, 1983.
- Bear, J., *Dynamics of Fluids in Porous Media*, Elsevier Sci., New York, 1972.
- Bello, M. S., R. Rezzonico, and P. G. Righetti, Use of Taylor-Aris dispersion for measurement of a solute diffusion coefficient in thin capillaries, *Science*, 266(5186), 773–776, 1994.
- Belongia, B. M., and J. C. Baygents, Measurements on the diffusion coefficient of colloidal particles by Taylor-Aris dispersion, *J. Colloid Interface Sci.*, 195(1), 19–31, 1997.
- Blackwell, R. J., Laboratory study of microscopic dispersion phenomena, *Soc. Pet. Eng. J.*, 2, 1–8, 1962.
- Brenner, H., Dispersion resulting from flow through spatially periodic porous media, *Philos. Trans. R. Soc. London, Ser. A*, 297, 81–133, 1980a.
- Brenner, H., A general theory of Taylor dispersion phenomena, *PhysicoChem. Hydrodyn.*, 1, 91–123, 1980b.
- Brenner, H., and D. A. Edwards, *Macrotransport Processes*, Butterworth-Heinemann, Woburn, Mass., 1993.
- Chen, J. S., C. S. Chen, H. S. Gau, and C. W. Liu, A two-well method to evaluate transverse dispersivity for tracer tests in a radially convergent flow field, *J. Hydrol.*, 223(3–4), 175–197, 1999.
- Cirpka, O. A., and P. K. Kitanidis, Characterization of mixing and dilution in heterogeneous aquifers by means of local temporal moments, *Water Resour. Res.*, 36(5), 1221–1236, 2000.
- Dagan, G., Time-dependent macrodispersion for solute transport in anisotropic heterogeneous aquifers, *Water Resour. Res.*, 24(9), 1491–1500, 1988.
- Fiori, A., and G. Dagan, Concentration fluctuations in aquifer transport: A rigorous first-order solution and applications, *J. Contam. Hydrol.*, 45(1–2), 139–163, 2000.
- Gelhar, L. W., and C. L. Axness, Three-dimensional stochastic analysis of macrodispersion in aquifers, *Water Resour. Res.*, 19(1), 161–180, 1983.
- Gelhar, L. W., C. Welty, and K. R. Rehfeldt, A critical review of data on field-scale dispersion in aquifers, *Water Resour. Res.*, 28(7), 1955–1974, 1992.
- Grane, F. E., and G. H. F. Gardner, Measurements of transverse dispersion in granular media, *J. Chem. Eng. Data*, 6(2), 283–287, 1961.
- Harleman, D. R. F., and R. R. Rumer, Longitudinal and lateral dispersion in an isotropic porous medium, *J. Fluid Mech.*, 16, 385–394, 1963.
- Hassinger, R. C., and D. U. V. Rosenberg, A mathematical and experimental examination of transverse dispersion coefficients, *Soc. Petrol. Eng. J.*, 8, 195–204, 1968.
- Kapoor, V., and L. W. Gelhar, Transport in three-dimensionally heterogeneous aquifers, 1, Dynamics of concentration fluctuations, *Water Resour. Res.*, 30(6), 1775–1788, 1994.
- Kapoor, V., and P. K. Kitanidis, Concentration fluctuations and dilution in two-dimensionally periodic heterogeneous porous media, *Transp. Porous Media*, 22, 91–119, 1996.
- Kapoor, V., and P. K. Kitanidis, Concentration fluctuations and dilution in aquifers, *Water Resour. Res.*, 34(5), 1181–1193, 1998.
- Kitanidis, P. K., Analysis of macrodispersion through volume-averaging: Moment equations, *Stoch. Hydrol. Hydraul.*, 6(1), 5–25, 1992.
- Kitanidis, P. K., The concept of the dilution index, *Water Resour. Res.*, 30(7), 2011–2026, 1994.
- Nadim, A., Measurement of shear-induced diffusion in concentrated suspensions with a Couette device, *Phys. Fluids*, 31(10), 2781–2785, 1988.
- Nishigaki, M., T. Sudinka, Y. Sasaki, M. Inoue, and T. Moriwaki, Laboratory determination of transverse and longitudinal dispersion coefficients in porous media, *J. Groundwater Hydrol.*, 38(1), 13–27, 1996.
- Oya, S., and A. J. Valocchi, Transport and biodegradation of solutes in stratified aquifers under enhanced in-situ bioremediation conditions, *Water Resour. Res.*, 34(12), 3323–3334, 1998.
- Perkins, T. K., and O. C. Johnston, A review of diffusion and dispersion in porous media, *Soc. Petrol. Eng. J.*, 3, 70–84, 1963.
- Perkins, T. K., O. C. Johnston, and R. N. Hofman, Mechanics of viscous fingering in miscible systems, *Soc. Petrol. Eng. J.*, 5, 301–317, 1965.
- Pisani, S., and N. Tosi, Two methods for the laboratory identification of transversal dispersivity, *Ground Water*, 32(3), 421–438, 1994.
- Robbins, G. A., Methods for determining transverse dispersion coefficients of porous media in laboratory column experiments, *Water Resour. Res.*, 25(6), 1249–1258, 1989.
- Scheidegger, A. E., General theory of dispersion in porous media, *J. Geophys. Res.*, 66(10), 3273–3278, 1961.
- Simpson, E. S., Transverse dispersion in liquid flow through porous media, Prof. Pap. 411-C, U.S. Geol. Surv., Washington, D.C., 1962.
- Taylor, G. I., Dispersion of soluble matter in solvent flowing slowly through a tube, *Proc. R. Soc. London, Ser. A*, 219, 186–203, 1953.
- Wang, J., and P. K. Kitanidis, Analysis of macrodispersion through volume averaging: comparison with stochastic theory, *Stoch. Environ. Res. Risk Assess.*, 13(1–2), 66–84, 1999.
- Zou, S., and A. Parr, Estimation of dispersion parameters for two-dimensional plumes, *Ground Water*, 31(3), 389–392, 1993.
- Zou, S., and A. Parr, Two-dimensional dispersivity estimation using tracer experiment data, *Ground Water*, 32(3), 367–373, 1994.

O. A. Cirpka, Universität Stuttgart, Institut für Wasserbau, 70550 Stuttgart, Germany. (olaf.cirpka@iws.uni-stuttgart.de)

P. K. Kitanidis, Department of Civil and Environmental Engineering, Stanford University, Stanford, CA 94305.

(Received May 8, 2000; revised October 2, 2000; accepted October 2, 2000.)